# Dynamical scaling of sputter-roughened surfaces in 2+1 dimensions

E. S. Tok,[1] S. W. Ong,[2] and H. C. Kang[2,*]
[1]*Department of Materials Science, National University of Singapore, 3 Science Drive 3, National University of Singapore, Singapore 117543*
[2]*Department of Chemistry, National University of Singapore, 3 Science Drive 3, National University of Singapore, Singapore 117543*
(Received 18 November 2003; revised manuscript received 26 April 2004; published 26 July 2004)

The asymptotic scaling behavior of sputter-roughened surfaces is of great current interest. In particular, the disparately wide-ranging values of the growth exponent found experimentally, and whether sputter-roughening belongs to the Kardar–Parisi–Zhang universality class in 2+1 dimensions, are two interesting issues. We address these issues using simulations of an atomistic model. The asymptotic scaling appears to be Edwards–Wilkinson. Crossover behavior in the model leads to *effective* growth exponents that vary widely depending upon the regime of observation.

DOI: 10.1103/PhysRevE.70.011604 PACS number(s): 68.35.Ct, 05.70.Ln, 68.35.Fx

Dynamical scaling ideas have been extensively applied to evolving interfaces using the general idea that the width of an interface depends in a self-affine manner upon the length and time as $w_l(t) \sim l^{\alpha} f(t/l^z)$ [1–5]. For large values of $t/l^z$, $f(t/l^z)$ goes to a constant and for $t/l^z$ much smaller than unity $f(t/l^z) \sim (t/l^z)^{\beta}$. The exponent $z$ is equal to $\alpha/\beta$. Thus, when $t/l^z$ is large, the roughness $w_l$ scales as $w_l \sim l^{\alpha}$ with the lateral length scale $l$. Similarly, the width grows as $w_l \sim t^{\beta}$ when $t/l^z$ is small. This dynamical scaling behavior is observed for rather diverse growth phenomena such as the evolution of flame fronts, chemical waves, and dendrites. It is also deeply related to other phenomena such as the properties of directed polymers in a random medium and the asymptotic mixing behavior of randomly stirred fluids. It has been proposed [6] that the asymptotic scaling properties for all these phenomena belong to the same universality class described by the Kardar–Parisi–Zhang (KPZ) equation

$$\frac{\partial h}{\partial t} = \nu \nabla^2 h + \frac{\lambda}{2} |\nabla h|^2 + \eta,$$

where $\nu$ is an effective surface tension. The nonlinear term arises because interfaces do not evolve merely by uniform displacement perpendicular to the plane of the interface; the global growth velocity of the interface is only the vertical component of the locally normal growth velocity of the interface. Taking this into account and keeping only the lowest-order term results in the nonlinear term above [6]. The delta-function correlated noise describing, for example, deposition or removal at random locations on the surface is given by the term $\eta$ with $\langle \eta(x,t)\eta(x',t') \rangle = D\delta(x-x')\delta(t-t')$ where $D$ is proportional to the sputtering flux.

There is evidence for KPZ scaling behavior for a wide-range of phenomena [1–5]. However, in the case of sputter-roughening of surfaces there are still unresolved questions about the asymptotic scaling properties of the interface. The evolution of a surface as a result of sputtering can be described by the Kuramoto–Sivashinsky (KS) equation [7]:

$$\frac{\partial h}{\partial t} = \nu \nabla^2 h + \frac{\lambda}{2} |\nabla h|^2 - \kappa \nabla^4 h + \eta.$$

In contrast to the KPZ equation, the bare value of the effective surface tension $\nu$ in the KS equation is negative. This negative surface tension, and the presence of the first two terms $\nabla^2 h$ and $|\nabla h|^2$, are the consequences of the atomic mechanism for roughening proposed by Sigmund [9], i.e., a sputtering particle dissipates its kinetic energy (through a collision cascade) in a Gaussian distribution centered about a point that is a finite distance beneath the point of impact at the surface of the solid. Generally, deriving the continuum equation from a microscopic model for interface growth/erosion is not a solved problem, but for the sputtering mechanism proposed by Sigmund, the continuum equation has been derived from the microscopic model. The KS equation has been shown [7,8] to include the lowest-order terms modelling this microscopic mechanism. Since the center of the energy dissipation distribution is beneath the surface sputter-erosion at the bottom of a valley is favored over sputter-erosion at the top of a hill [7,8]. The $-\kappa \nabla^4 h$ term describes chemical-potential gradient driven diffusive surface relaxation [10], and in combination with a negative $\nu$ determines a cutoff-wave vector below which surface height fluctuations are not stable [11]. On the other hand the nonlinear term in the KS equation serves to couple modes with different wave vectors stabilizing the height fluctuations [12]. In the case of 1+1 dimensions, analytic argument shows that the asymptotic scaling behavior of the KS equation is the same as that for the KPZ equation [13]. Numerical simulations verify this conclusion [14,15]. However, in the case of 2+1 dimensions, which is the important case for the study of sputter-roughened solid surfaces, direct numerical simulations have not been conclusive [16]. Similarly, analytic treatments by different groups have led to different conclusions [13,17]. Thus, there is no consensus on the asymptotic scaling behavior of the KS equation for 2+1 dimensions. Aside from the question of whether the asymptotic behavior for the KS equation is in the KPZ universality class,

*Corresponding author.

 

it is also interesting to study the scaling behavior for early or intermediate times, and to see how these might crossover to late-time behavior. This is particularly relevant to the analysis of experimental data where, for instance, growth exponents ranging from 0.1 [18] to unity [19] have been reported. It is not straightforward to establish if two different experiments probe the same time or length regimes of the roughening behavior, and the range of experimentally observed growth exponents may well be due to the different time scales probed in different experiments. The purpose of this work is to attempt an atomistic simulation of the sputtering process in order to contribute to the discussion of these issues.

Our atomistic model uses particles arranged in a simple cubic lattice to simulate the solid. Only results for the sputtering flux in the direction normal to the (horizontal) surface plane of $N=N_x\times N_y$ sites are reported here. When a sputtering particle hits the surface, the probability of a surface particle being ejected is computed using a Gaussian distribution centered at a point at depth $d$ vertically below the surface site at which impact occurs. For each iteration, the lattice position in the horizontal plane at which the sputtering particle hits the surface is chosen at random. Thus, the atomic mechanism for sputtering in our model is exactly that proposed by Sigmund [9] and shown [7,8] to be described, in the lowest approximation, by the first two terms of the KS equation above. Nearest-neighbor and next-nearest-neighbor particle pairs have attractive interactions of equal strength $J$. Both thermally activated diffusion and sputtering moves are allowed. In each iteration of the Monte Carlo simulation, either a diffusion event or a sputtering event is attempted. The choice is governed by a parameter $p$; the probability of attempting a sputtering event is equal to $pN/(pN+N_a)$ where $N_a$ is the number of active particles. An active particle is a particle that has at least one vacant nearest-neighbor or next-nearest-neighbor site to which it can migrate. The parameter $p$ is the ratio of the attempt rate for a sputtering event per site to the attempt rate (set to unity) for diffusion of an active particle. Thus, the probability $pN/(pN+N_a)$ is the ratio of the overall rate at which sputtering *attempts* occur to the overall rate of diffusion attempts. The time-step in each iteration is given by the quantity $1/(pN+N_a)$. The number of active sites changes as the surface roughens; thus in our simulations each Monte Carlo iteration corresponds to a time-step of varying length. Each simulation corresponds to a constant sputtering flux determined by $p$. If a sputtering attempt is chosen, a point of impact on the surface accessible to a vertical trajectory is randomly selected. A solid particle is selected according to a Gaussian distribution of width $\sigma$ centered at depth $d$ vertically below the point of impact. If the selected particle is an active particle, it is ejected and removed from the solid. Otherwise the iteration ends. If a diffusion attempt occurs, an active particle is randomly selected from the list of all active particles. A Metropolis [20] scheme is used to decide if the migration of the selected particle to a randomly selected vacant neighboring site is successful. A temperature $T$ is used to control the success rate of the attempted diffusive moves. Clearly $T$ must be set sufficiently low in order for the solid not to melt or evaporate. On the other hand, if $T$ is too low, diffusion attempts are rarely successful and the rate of thermal diffusion is reduced.

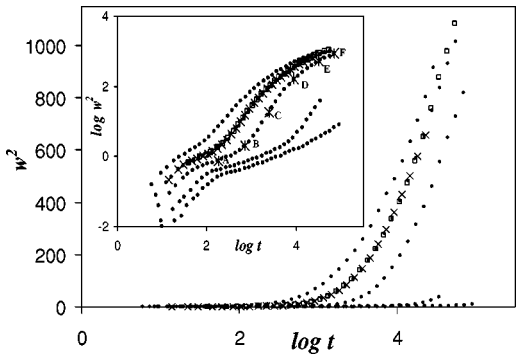


FIG. 1. This figure shows plots of $w^2$ vs. log $t$ for $J/k_BT=0.5$. The same data is plotted in the inset as log $w^2$ vs. log $t$. In both the main and the inset panels, the data shown is for $p=0.1$, 0.05, 0.025, 0.01, and 0.005 in order of decreasing roughness for each value of time. Data for $50\times50$ (squares), $100\times100$ (dots), and $400\times400$ (crosses) lattices are shown for $p=0.05$. Data for the $100\times100$ lattices is averaged over five runs, and that for the $50\times50$ lattice is averaged over eight runs. The labeled crosses for $p=0.025$ are data points corresponding to the height and height-correlation maps in Figs. 3 and 4.

Using this model we investigate the effects of varying the relative rates of sputtering to diffusion. Plots of the interface width $w$ as a function of time $t$ are shown in Fig. 1. The value of $p$ is varied from 0.005 to 0.1. This set of data is mainly from simulations with a substrate lattice size of $N_x\times N_y=100\times100$, although we also include data for lattice sizes $400\times400$ and $50\times50$ for $p=0.05$. The depth parameter $d$ is set at unity. This means that the center of the Gaussian distribution used to select a particle to sputter off the surface is one lattice constant below the surface particle at which impact occurs. The temperature for the data shown in Fig. 1 is chosen so that $J/k_BT$ is equal to 0.5. The corresponding data for $J/k_BT=5.0$ is shown in Fig. 2. In each of these figures, the inset shows the same data plotted as log $w^2$ vs. log $t$. For all the results reported here the width $\sigma$ of the Gaussian distribution for energy dissipation is set at one lattice constant.

There is a short early time regime in which the initially atomically smooth surface rapidly roughens for very small values of roughness; for $J/k_BT$ equal to 0.5, the surface roughness is smaller than one for this regime. Hence, this is regime is probably not of relevance to actual sputtering experiments. When the attempt rate for sputtering is small there is an intermediate regime in which the growth kinetics is considerably slower than the initial regime. For small values of $p$ this intermediate regime is clearly defined in the log $w^2$ vs. log $t$ plots. However, the duration of this intermediate regime decreases as $p$ increases, and for the $p=0.1$ data in Fig. 1 (inset) this intermediate regime is barely discernible. Assuming power-law kinetics $w\sim t^{\beta}$, the effective $\beta$ value after the "knee" of each curve in Fig. 1 slowly increases from approximately $0.17\pm0.02$ for $p=0.005$ to approximately $0.35\pm0.02$ for $p=0.1$. The error margins reported here and elsewhere in the paper are obtained by analyzing the results of two independent sets of simulations with the same number of runs. We want to emphasize that in the intermediate scaling regime these exponents are effective exponents in the

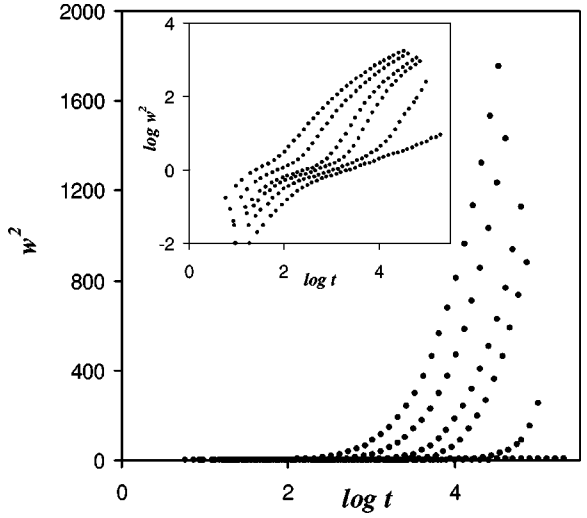


FIG. 2. This figure shows plots of $w^2$ vs. log $t$ for $J/k_BT=5.0$. The same data is plotted in the inset as log $w^2$ vs. log $t$. As in Fig. 1, in both the main and the inset panels, the data shown is for $p=0.1, 0.05, 0.025, 0.01$, and 0.005 in order of decreasing roughness for each value of time. In contrast with Fig. 1, the asymptotic logarithmic regime is not as clearly established here.

sense that the growth kinetics is only effectively power-law. The data also shows a slow increase of the effective $\beta$ value with $p$ in this intermediate regime. The $J/k_BT=5.0$ data in Fig. 2 shows a similar increase from $\beta=0.18\pm0.02$ for $p=0.005$ to $\beta=0.38\pm0.01$ for $p=0.1$. From the data for the smallest sputtering flux ($p=0.005$) in Fig. 1, it appears that the effective value of $\beta$ slowly increases in the intermediate time regime for $J/k_BT=0.5$. It does not appear that the power-law scaling holds for much more than one decade of time. For $J/k_BT=5.0$ a longer duration is observed in which an *effective* power-law scaling applies, but all our data for this intermediate regime supports the suggestion that power-law scaling does not hold for the KS equation in $2+1$ dimensions [21]. The largest interface width in our simulations is slightly larger than 30 for a $100\times100$ lattice. In this growth regime the roughness is quite large and a cellular surface morphology is clearly observed. This is illustrated in Figs. 3 and 4. Contour plots of the surface height at various times is shown in Fig. 3 for a $(100\times100)$ lattice. These maps of the surface heights correspond to the $p=0.025$ roughening kinetics data plotted in Fig. 1. The corresponding simulation time for each of these height maps is indicated by a labeled cross in Fig. 1. We used contour lines to indicate heights that are equal to or lower (higher) than 25 (75)% of the range between the lowest and the highest points on the surface for each of these maps. The gradual roughening with time can be observed; the rather uniform spacing of the contour lines at the sides of the "hills" or "basins" shows that these are somewhat conical in shape. The tops of the "hills" appear to be slightly flattened.

In addition to the height-maps, we also plot maps of the height-height correlation $g(\vec{r},t)=\langle h(\vec{r},t)h(\vec{0},t)\rangle$ in Fig. 4. These maps correspond to the height-maps plotted in Fig. 3. Here, contour lines indicate height correlations from 75% to 100% of the maximum peak (at the origin). These maps

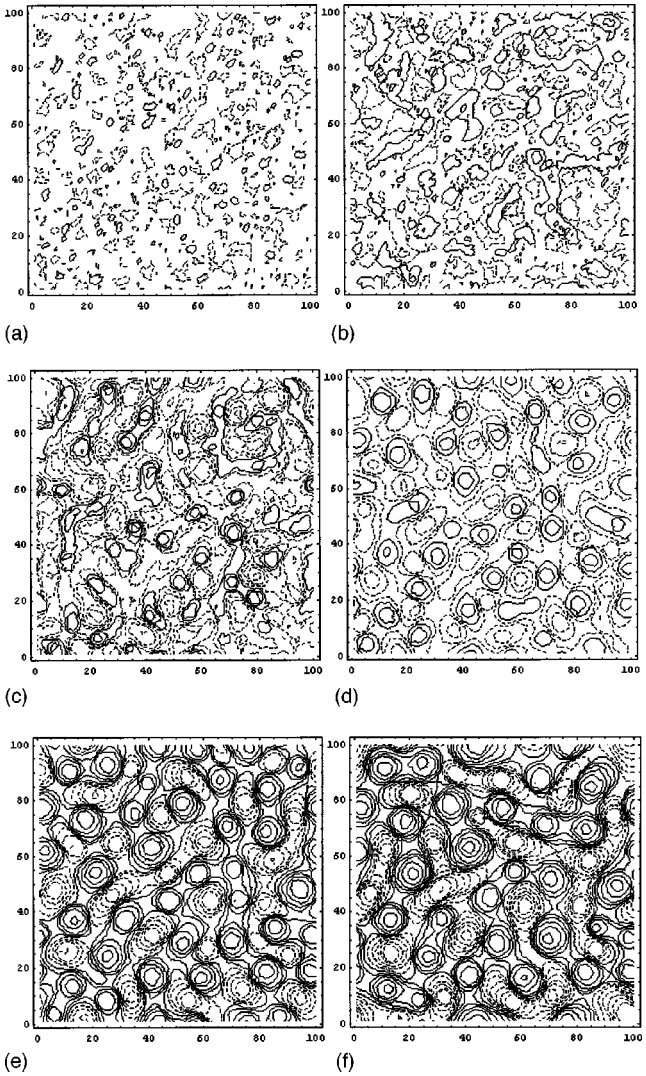


FIG. 3. The surface configurations corresponding to the labeled crosses for the $p=0.025$ run in Fig. 1 are plotted here. Dashed (solid) lines are contours for heights that are higher (lower) than or equal to 50% of the range between the lowest and the highest point for each plot. The contour spacing used in each plot is fixed. These are two units for plots (a) and (b), three units for (c), and ten units for plots (d)–(f).

show that a hexagonal symmetry develops with sputtering as has been previously observed experimentally [22]. Straight lines are drawn to indicate the positions of the first-order maxima in the height-height correlation. The positions of these maxima show that the widths of the "hills" and "basins" on the surface increase gradually with time.

From the main panel in Fig. 1 the data for $p=0.1$ and 0.05 show that the growth kinetics at late times scales as $w^2 \sim \log t$. That is, Edwards–Wilkinson behavior [23] is observed. For $p=0.05$ and $J/k_BT=0.5$, the value of the effective exponent at the longest time is approximately $0.15\pm0.01$, i.e., it is already considerably smaller than the KPZ growth exponent in $2+1$ dimensions; that is asymptotic sputtering kinetics is Edwards–Wilkinson rather than KPZ. These observations support the suggestion that in $2+1$ dimensions, the asymptotic scaling behavior for the KS equa-

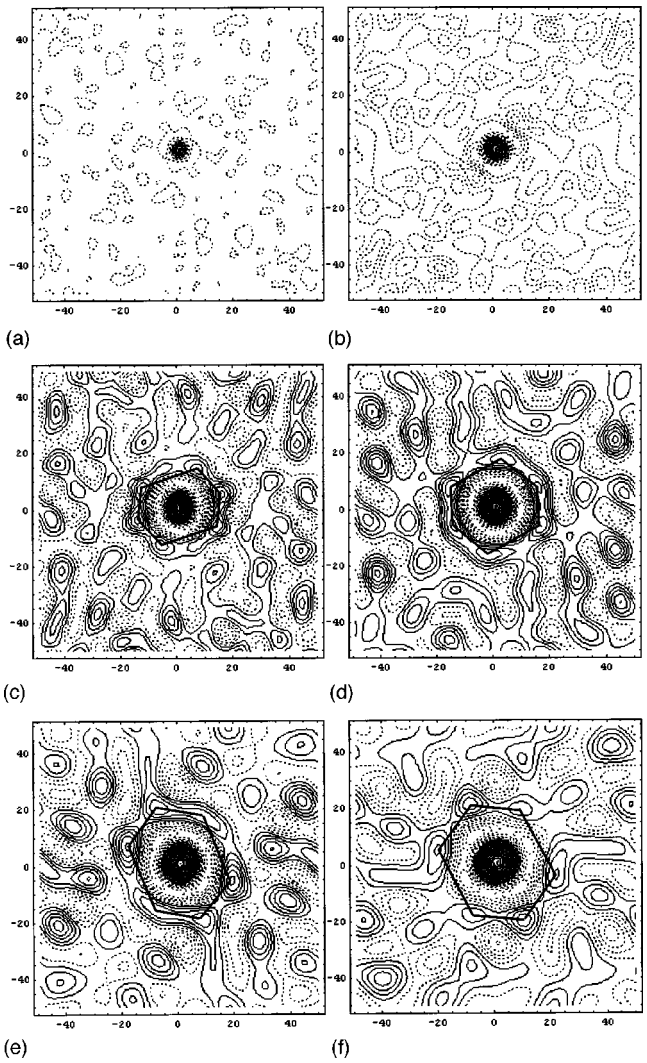


FIG. 4. The height-correlations $g(\vec{r},t)=\langle h(\vec{r},t)h(\vec{0},t)\rangle$ corresponding to the surface configurations shown in Fig. 3 are plotted here. Solid (dashed) contours indicate correlations higher (lower) than 0.75 of the maximum for each plot. The contour spacing used in each plot is fixed. These are 0.05, 0.1, 0.75, 7.5, 25, and 40 in order of increasing time. The straight lines are drawn to indicate the positions of the first-order maxima in the correlation.

tion is not KPZ. This is more clearly so for the higher temperature data. The plot in the main panel of Fig. 2 shows that the EW scaling regime is just barely reached in our $J/k_BT=5.0$ simulations. Thus, as the temperature is lowered and the diffusion rate decreases, the asymptotic regime EW is reached at larger length and time scales. The simulation results we have described above provide a framework for understanding the wide-ranging values of $\beta$ that are obtained from various experimental measurements. Low $\beta$ values can be understood in two ways. If the growth has reached the EW regime, then the effective value of the growth exponent may be small. In our longest simulations, a value of $0.15\pm0.01$ was observed. This corresponds to the long-time and large-$p$ of the data shown in Fig. 1, i.e., large sputtering flux relative to diffusion rate. On the other hand, a small value of $\beta$ may also be observed if the experiment probes the intermediate growth regime for a system with a small value of $p$; as noted above, the duration of this intermediate regime increases as $p$ decreases, i.e., small sputtering flux compared to diffusion rate. The simulations show that the effective value of $\beta$ in this regime decreases as $p$ decreases. However, it is not clear from our simulations if there is a nonzero asymptotic value of $\beta$ in the low $p$ limit. The smallest value that we observed is approximately $0.17\pm0.02$.

The high $\beta$ values reported in experiments can be understood as corresponding to the crossover from the intermediate growth regime to the EW regime. For the curves shown in the inset of Fig. 1 (Fig. 2) the effective value of $\beta$ for this crossover region ranges from 0.74 (0.79) to 1.0 (1.1) for $J/k_BT=0.5$ (5.0). The data for $p$ equal to 0.025 and 0.0175 suggest an upper bound of 1.0 for this effective $\beta$ value; somewhat longer simulation runs for lower $p$ values are needed to confirm this upper bound. In summary, depending upon the time regime probed, the data shows that a wide range of effective $\beta$ values (up to unity) may be observed.

Direct numerical integration [14] and atomistic simulation [24] have previously been used to study sputter erosion. Comparing our data in Figs. 1 and 2 to the time dependence of the interface width in Ref. [14] (Figs. 10 and 12), it appears that Ref. [14] observed growth kinetics that is similar to what we observe here as the intermediate time regime and the early part of the crossover to EW behavior. The different kinetic regimes we observed are also seen in the atomistic simulations of Ref. [24] (Fig. 4) although the rapid increase in the interface width at the end of the intermediate regime was attributed to finite-size effects there. Our data for the $400\times400$ and $50\times50$ lattices plotted in Fig. 1 demonstrate that this is probably not the case; there is no indication of a finite-size effect for the regime that we have probed in the simulations. We also show that varying the parameter $p$ varies the duration of the intermediate regime. In Fig. 2, the smallest value of $p$ results in an intermediate regime that covers more than two decades of time. Our results suggest that the crossover from the intermediate regime to EW scaling corresponds to roughening dominated by the stabilizing nonlinear term to roughening dominated by the linear terms in the KS equation. The kinetics in the intermediate region is only *effectively* power-law; except for smallest value of $p$ this is clearly seen in the data in the insets of Figs. 1 and 2.

In order to investigate the scaling behavior further, the roughness exponent $\alpha$ is obtained by computing the width of the interface as a function of the horizontal length scale $l$. For each lattice size $L=L_x=N_y$, box sizes ranging from $l=2$ to $l=L$ are used to measure $w_l$. The data for a $400\times400$ lattice is plotted in Fig. 5. This data (inset) shows that for short-length scales, the interface width $w_l$ scales linearly with the length, that is, $w_l\sim l^\alpha$ with $\alpha$ equal to unity. The plots in Fig. 5 show the expected finite-size effect such that for sufficiently long lengths $l$, the roughness $w_l$ reaches a saturation value. However, for an intermediate length regime, a distinctly linear dependence of $w_l^2$ upon the logarithm of $l$ is observed. This scaling regime is not observed for either very long times or very short times. In particular, it is not observed for the curve corresponding to the longest time in Fig. 5. The length scale over which $w_l\sim l$ slowly increases with time; at long times, only the $w_l\sim l$ regime and the saturated

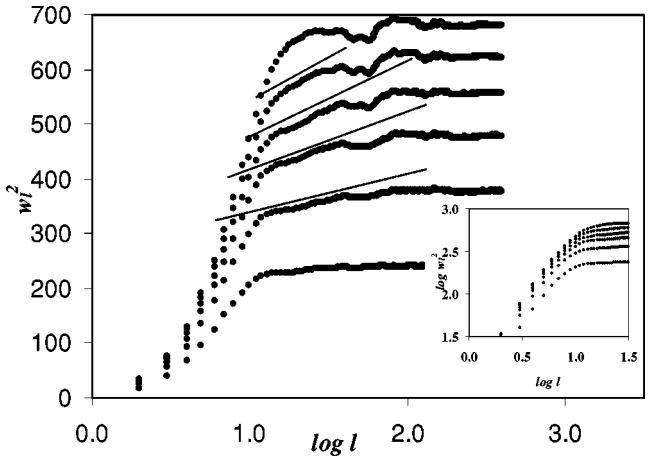


FIG. 5. This figure shows plots of $w_l^2$ vs $l$ for various values of time for $p=0.05$ and $J/k_BT=0.5$ for $400\times400$ lattices. Here $w_l$, the vertical length scale, is measured by determining the roughness of subsets of the lattice of size $l\times l$. In the inset log $w_l^2$ is plotted versus log $l$. The plots correspond, in order of increasing asymptotic roughness $w_l^2$, to $t=5810$, 9724, 13526, 17249, 20930 and 24469 units. This is data, averaged over three $400\times400$ lattice runs, for the same set of parameters as the $p=0.05$ data in Fig. 1.

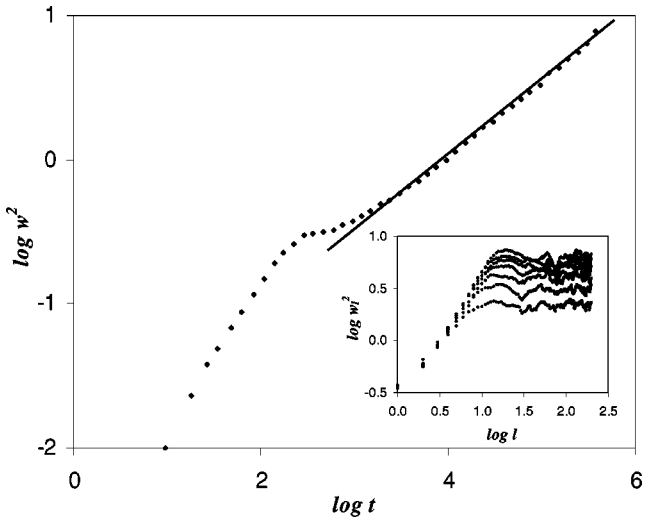


FIG. 6. This figure plots log $w^2$ vs log $t$ for $p=0.01$ and $J/k_BT=0.5$ when the center of the distribution for selecting particles to be sputtered is located *above* the point of impact. In the inset, the dependence of log $w_l^2$ upon log $l$ is plotted for the same simulation run. A KPZ growth exponent is clearly observed.

regime are observed. Similarly, we do not observe the logarithmic scaling regime for short times. We were also not able to observe this EW regime for smaller lattices of $200\times200$ suggesting that the asymptotic roughening behavior can be seen only at somewhat large lateral lengths.

The linear scaling $w_l\sim l$ for short lengths is understandable if we consider the conical cellular structure of the interface observed in the simulations; the vertical length scale is linearly proportional to the lateral length scale when the latter is smaller than or on the order of the lateral size of the cones. This conical and cellular nature of the surface has been observed experimentally, and also suggested by theoretical considerations [25]. Our simulation results suggest the following scenario for sputter-roughening of infinitely large surfaces. A conical structure develops on the surface so that $w_l$ scales linearly with $l$ for small $l$ and for any time regime. At long times and long horizontal length scales, the roughening is EW; conical structures decorate a logarithmically rough surface with unstable long wavelength fluctutations. For finite-sized surfaces, the logarithmic scaling with lateral length scale is not easily accessible at long times because the roughness saturates at smaller horizontal lengths than is necessary for observing it. The results presented here are consistent with numerical work combined with perturbation theory [16] that suggests EW behavior at long time for the deterministic KS equation. Our simulations provide strong evidence that the asymptotic behavior of the KS equation in $2+1$ dimensions is not in the KPZ universality class.

An interesting point noted previously is that the bare value of the parameter $\nu$ in the KS equation becomes positive if the center of the Gaussian distribution for selecting particles to sputter is displaced above the point of impact [25]. With a positive value of $\nu$, the KPZ equation is recovered. Then, the growth exponent is expected to be approximately 0.24 and the cellular structures that develop on the surface are rounded bulges instead of cones. We investigate this by setting the depth parameter $d$ equal to $-1$, that is, the center of the Gaussian distribution for sputtering is one lattice constant *above* the site at which impact occurs. For $p=0.01$ and $J/k_BT=0.5$, the KPZ growth exponent is obtained ($w\sim t^\beta$; $\beta=0.24\pm0.02$) as shown in Fig. 6. The inset shows that $w_l\sim l^\alpha$ with $\alpha$ close to $\frac{1}{2}$. Thus, our simulations provide direct atomistic evidence for the relationship between the depth of the center for the distribution of sputtered particles and the sign of the effective surface tension.

In summary, the data reported here provide evidence for EW behavior in the long time limit for a sputter-eroded surface. The crossover to EW behavior occurs more slowly when diffusive surface relaxation is slow. For our longest simulations, the effective growth exponent is approximately $0.15\pm0.01$ and is clearly already lower than the KPZ value. Depending upon the time regime in which effective growth exponents are measured, a wide range of values (up to unity) may be obtained, consistent with what is observed experimentally. For the lowest values of $p$, we see an extended intermediate regime where the width is described by $w\sim t^\beta$. However, in general, the behavior observed in our intermediate regime is characterized by an *effective* $\beta$ that slowly increases with time. A cellular structure of conical "hills" and "basins" with hexagonal symmetry develops on the surface. While the growth kinetics is quite readily accessible, the roughness scaling is difficult to access in simulations presumably because of the large lateral length scales required. In addition, setting the depth parameter to a negative value changes the behavior to KPZ in agreement with previous analysis.

[1] J. Krug and H. Spohn, in *Solids Far from Equilibrium: Growth, Morphology and Defects*, edited by C. Godrèche (Cambridge University Press, Cambridge, England, 1991).
[2] *Dynamics of Fractal Surfaces*, edited by F. Family and T. Vicsek (World Scientific, Singapore, 1991).
[3] P. Meakin, Phys. Rep. **235**, 189 (1993).
[4] A. L. Barabási and H. E. Stanley, *Fractal Concepts in Surface Growth* (Cambridge University Press, Cambridge, England, 1995).
[5] T. Halpin-Healey and Y. C. Zhang, Phys. Rep. **254**, 215 (1995).
[6] M. Kardar, G. Parisi, and Y. C. Zhang, Phys. Rev. Lett. **56**, 889 (1986).
[7] R. Cuerno and A. L. Barabási, Phys. Rev. Lett. **74**, 4746 (1995).
[8] R. M. Bradley and J. M.E. Harper, J. Vac. Sci. Technol. A **6**, 2390 (1988).
[9] P. Sigmund, Phys. Rev. **184**, 383 (1969).
[10] S. Das Sarma and P. Tamborenea, Phys. Rev. Lett. **66**, 325 (1991).
[11] R. Cuerno and K. B. Lauritsen, Phys. Rev. E **52**, 4853 (1995).
[12] M. Rost and J. Krug, Physica D **88**, 1 (l995).
[13] C. Jayaprakash, F. Hayot, and R. Pandit, Phys. Rev. Lett. **71**, 12 (1993).
[14] K. Sneppen, J. Krug, M. H. Jensen, C. Jayaprakash, and T. Bohr, Phys. Rev. A **46**, R7351 (1992).
[15] R. Cuerno, H. A. Makse, S. Tomassone, S. T. Harrington, and H. E. Stanley, Phys. Rev. Lett. **75**, 4464 (1995).
[16] J. T. Drotar, Y. P. Zhao, T. M. Lu, and G. C. Wang, Phys. Rev. E **59**, 177 (1999).
[17] V. S. L'vov and I. Procaccia, Phys. Rev. Lett. **69**, 3543 (1992).
[18] D. M. Smiligies, P. J. Eng, E. Landemark, and M. Nielsen, Europhys. Lett. **38**, 447 (1997).
[19] E. Chason and T. M. Mayer, Appl. Phys. Lett. **62**, 363 (1993).
[20] N. Metropolis, A. W. Rosenbluth, M. N. Rosenbluth, A. H. Teller, and E. Teller, J. Chem. Phys. **21**, 1087 (1953).
[21] I. Procaccia, M. H. Jensen, V. S. L'vov, K. Sneppen, and R. Zeitak, Phys. Rev. A **46**, 3220 (1992).
[22] S. Facsko, T. Dekorsy, C. Koerdt, C. Trappe, H. Kurz, A. Vogt, and H. L. Hartnagel, Science **285**, 1551 (1999).
[23] S. F. Edwards and D. R. Wilkinson, Proc. R. Soc. London, Ser. A **381**, 17 (1982).
[24] A. K. Hartmann, R. Kree, U. Geyer, and M. Kölbel, Phys. Rev. B **65**, 193403 (2002).
[25] R. M. Bradley, Phys. Rev. E **54**, 6149 (1996).